European Journal of Pharmaceutics and Biopharmaceutics 192 (2023) 79–87

Contents lists available at ScienceDirect

European Journal of Pharmaceutics and Biopharmaceutics

journal homepage: www.elsevier.com/locate/ejpb

Research paper

Site-specific PEGylation of recombinant tissue-type plasminogen activator

Kirstin Meiners [a], Prisca Hamm [a], Marcus Gutmann [a], Jan Niedens [b], Agnieszka Nowak-Król [b], Salvador Pané [c], Tessa Lühmann [a,*]

[a] Institute of Pharmacy and Food Chemistry, University of Würzburg, Am Hubland, DE-97074 Würzburg, Germany
[b] Institute of Inorganic Chemistry and Institute for Sustainable Chemistry & Catalysis with Boron, University of Würzburg, Am Hubland, DE-97074 Würzburg, Germany
[c] Multi-Scale Robotics Lab (MSRL), Institute of Robotics & Intelligent Systems (IRIS), ETH Zürich, CH-8092 Zürich, Switzerland

ARTICLE INFO

Keywords:
Tissue-type plasminogen activator
PEGylation
Ischemic stroke
Plasminogen activator inhibitor-1

ABSTRACT

Tissue-type plasminogen activator (tPA) is the gold standard for emergency treatment of ischemic stroke, which is the third leading cause of death worldwide. Major challenges of tPA therapy are its rapid elimination by plasminogen activator inhibitor-1 (PAI-1) and hepatic clearance, leading to the use of high doses and consequent serious side effects, including internal bleeding, swelling and low blood pressure. In this regard, we developed three polyethylene glycol (PEG)ylated tPA bioconjugates based on the recombinant human tPA drug Alteplase using site-specific conjugation strategies. The first bioconjugate with PEGylation at the N-terminus of tPA performed by reductive alkylation showed a reduced proteolytic activity of 68 % compared to wild type tPA. PEGylation at the single-free cysteine of tPA with linear and branched PEG revealed similar proteolytic activities as the wild-type protein. Moreover, both bioconjugates with PEG-cysteine-modification showed 2-fold slower inhibition kinetics by PAI-1. All bioconjugates increased in hydrodynamic size as a critical requirement for half-life extension.

1. Introduction

Human tissue-type plasminogen activator (tPA) is a serine protease (MW 65 kDa) catalyzing the fibrin-enhanced activation of plasminogen to the active serine protease plasmin by cleaving its Arg561-Val562 peptide bond [1,2]. Plasmin is responsible for the dissolution of blood clots by degrading fibrin structures and thus is physiologically involved in the balance between coagulation and fibrinolysis [3]. tPA is therefore used in the treatment of ischemic stroke to indirectly dissolve the occluding thrombus. Thereby, tPA is administered in high doses (0.9 mg tPA per kg body weight) due to hepatic clearance with half-life about 3 min and rapid inactivation by endogenous plasminogen activator inhibitor-1 (PAI-1) [4–7]. This in turn, leads to serious side effects such as bleeding complications and intracerebral hemorrhage and makes it necessary to properly evaluate the risk–benefit ratio [8].

Substantial efforts were made to develop novel thrombolytics by mutations, such as Tenecteplase, to decrease the inhibition by PAI-1. Unfortunately, this mutant of human tPA resulted in a higher risk of internal bleeding and to date, recombinant tissue-type plasminogen activator is the only U.S. Food and Drug Administration (FDA) approved thrombolytic drug for the treatment of acute ischemic stroke, recommended for its ability to achieve early reperfusion and improve neurological outcomes [4,9,10].

An FDA approved strategy to prolong serum half-life and reduce protein interactions comprises the covalent conjugation of the protein's surface with hydrophilic polymers such as polyethylene glycol (PEG). To induce steric hindrance, Mu et al. prepared PEGylated staphylokinase by varying the length of the PEG chain and the PEGylation site on the protein's surface. The used PEG polymers of a size up to 20 kDa formed a hydrated layer with steric shielding effects to mask interacting amino acids at its binding site of the receptor [11,12].

Two different strategies are available to achieve site-specific PEGylations on endogenous proteins [13,14]. First, the N-terminus can be selectively targeted at pH 5 by reductive amination since the α-amine has a lower pKa than the ε-amine of the lysine residues [15]. Nevertheless, complete selectivity cannot be obtained, but the heterogeneity often observed when targeting lysine residues is highly reduced [16]. We previously performed selective N-terminal modification with PEG and PEG alternative polymers of human interleukin-4 and vascular endothelial growth factor 165 ($VEGF_{165}$), demonstrating site-selectivity and high bioactivity of the PEGylated product [17,18].

Another site-specific strategy deploys free cysteine residue accessible

* Corresponding author at: Institute of Pharmacy and Food Chemistry, University of Wuerzburg, Am Hubland, DE-97074 Wuerzburg, Germany.
E-mail address: tessa.luehmann@uni-wuerzburg.de (T. Lühmann).

https://doi.org/10.1016/j.ejpb.2023.09.017
Received 6 July 2023; Received in revised form 13 September 2023; Accepted 29 September 2023
Available online 30 September 2023

on the protein's surface with maleimides to form thioether conjugates. As cysteines are less present on the surface of proteins and are often involved in disulfide bridges, selectivity can be achieved in this way [16]. However, this approach also poses challenges, such as instabilities derived from hydrolysis of the thioether bond or exchange reactions with free thiols e.g. of albumin within the blood after administration [13].

A previous study revealed a significant reduction of the proteolytic activity of tPA when non-specifically PEGylated using N-Hydroxysuccinimide (NHS) based chemistry [19]. Here, we aimed for site-specific PEGylation of the recombinant human tPA Alteplase using (i) reductive alkylation and (ii) maleimide chemistry, the latter with linear and branched PEG. Both approaches and the influence of the PEG architecture were compared regarding bioactivity and interaction of PEGylated tPA with its inhibitor PAI-1.

2. Material and methods

Recombinant tissue-type plasminogen activator (tPA) was purchased as lyophilized powder formulation (Actilyse® 50 mg, Alteplase for injection E.P., PZN 03300636) from Boehringer Ingelheim (Ingelheim am Rhein, Germany). According to the drug manufacturer, 1 mg tPA corresponds to 46.66 mg Actilyse® and 580,000 International Units (IU). Linear methoxy-polyethylene glycol functionalized with a single aldehyde group (mPEG-Ald) and an average mass of 20,000 g/mol was purchased by Iris Biotech GmbH (Marktredwitz, Germany). Linear methoxy-polyethylene glycol functionalized with a single maleimide group (mPEG-Mal) and an average mass of 20,000 g/mol was purchased from Merck KGaA (Darmstadt, Germany). 2-arm branched methoxy-polyethylene glycol functionalized with a single maleimide group (m-*b*PEG-Mal) and an average mass of 20,000 g/mol was purchased from NOF Corporation (Tokyo, Japan). Fluorescence substrate glutaryl-L-glycine-L-arginine-7-amino-4-methylcumarin-hydrochloride (Glutaryl-Gly-Arg-AMC, $>$ 99 %) was purchased by Bachem AG (Bubendorf, Switzerland). Chromogenic substrate methanesulfonyl-D-hexahydrotyrosine-L-glycine-L-arginine-p-nitroanilide-acetate (T2943, $\geq$ 95 %), human plasminogen activator inhibitor-1 (PAI-1, $\geq$ 98 %) and Dulbecco's modified Eagle's medium were purchased from Merck KGaA (Darmstadt, Germany). WST-1 was purchased from Roche Diagnostics GmbH (Mannheim, Germany). 4x NuPAGE Sample buffer and 4–20 % Tris-Glycine acrylamide gel were purchased from ThermoFisher Scientific (Karlsruhe, Germany). Deionized, purified water (Millipore water) was generated by a Millipore purification system from Merck KGaA (Darmstadt, Germany). All other reagents and laboratory consumables were purchased by Merck KGaA (Darmstadt, Germany) or VWR International GmbH (Ismaning, Germany) in at least biochemical grade, unless otherwise noted.

2.1. Synthesis of tPA PEGylated at the N-terminus

Site-specific conjugation of tPA with polyethylene glycol (PEG) at the N-terminus (Ser1) was achieved by reductive amination at pH 5 via a Schiff base intermediate with mPEG-Ald [20]. Therefore, 40 μM tPA in 0.1 M sodium acetate buffer pH 5 was dialyzed using Slide-A-Lyzer ® MINI with 3.5 kDa cut-off (ThermoFisher Scientific, Karlsruhe, Germany) against the same buffer for 40 h at 4 °C to remove interfering arginine and salts present in the formulation. The resulting pre-chilled protein solution was gently mixed with 15-fold molar excess of mPEG-Ald in the same buffer. The reaction was started by further addition of freshly prepared reducing agent sodium cyanoborohydride solution ($NaCNBH_3$) as reducing agent to a final concentration of 30 mM. The reaction mixture was gently shaken on a VWR OS-500 shaker (VWR International GmbH, Ismaning, Germany) for 40 h at 4 °C.

2.2. Synthesis of tPA PEGylated at a single-free cysteine

Site-specific modification of tPA with PEG at a single-free cysteine (Cys83) was performed by maleimide reaction. For this reason, 17 μM tPA in buffered saline (PBS) pH 7.4 was gently mixed with 15-fold molar excess of mPEG-Mal or m-*b*PEG- Mal in the same buffer. The reaction mixture was gently shaken on a VWR OS-500 shaker for 40 h at 4 °C. [21].

2.3. Purification of PEGylated tPA conjugates

The tPA conjugates PEGylated at the N-terminus (PEG-Ser1-tPA), at a single cysteine with linear PEG (PEG-Cys83-tPA) or branched PEG (*b*PEG-Cys83-tPA*)* were purified by cation exchange chromatography (CEX). For this purpose, the reaction mixtures were diluted 4-fold in 25 mM sodium acetate buffer pH 5 respectively and subsequently loaded on a FPLC system (ÄKTA pure) equipped with two HiTrap™ SP HP 1 mL columns (Cytiva, Freiburg, Germany) with a flow rate of 1 mL/min. For elution, the NaCl concentration was linearly increased from 0 % to 40 % in 12 column volumes using 25 mM sodium acetate buffer pH 5 with 2 M NaCl. The fractions with mono-conjugated tPA were identified with SDS-Page analysis and rebuffered against PBS pH 7.4 using Slide-A-Lyzer ® MINI with 3.5 kDa cut-off.

2.4. SDS-page analysis

Sodium dodecyl sulfate–polyacrylamide gel electrophoresis was performed under reductive conditions. For this, samples were mixed with solubilization buffer (250 mM Tris-HCl pH 8.0, 7.5 % w/v SDS, 25 % v/v glycerol, 0.25 mg/mL bromophenol blue, 12.5 % v/v β-mercaptoethanol) and incubated at 95 °C for 5 min. SDS-Page was performed using 37.5 mM Tris-HCl with 1 g/L SDS for stacking (pH 6.8) and separating gel (pH 8.8), the latter with 12 % acrylamide. 25 mM Tris-HCl with 192 mM glycine and 1 g/L SDS was used as running buffer. Staining was performed with Coomassie blue G-250 solution.

2.5. Size exclusion chromatography

Purities of PEGylated tPA variants were analyzed on an Agilent 1260 infinity II HPLC (Agilent Technologies Inc., Waldbronn, Germany) using a TSKgel G300SW 10 μm 600 × 7,5 mm size exclusion (SEC) column (Tosoh Bioscience GmbH, Griesheim, Germany). The device was equipped with a variable wavelength detector (G7115A, Agilent), an automatic vial sampler (G7129C, Agilent), a pump (G7104C, Agilent), and a multicolumn oven (G7116A, Agilent). Mobile phase was 30 g/L sodium dihydrogen phosphate and 1 g/L sodium dodecyl sulfate (SDS) pH 6.8 in Millipore water with an isocratic flow of 0.5 mL/min for 60 min. The injection volume was 50 μL and the detector was set to a wavelength of 214 nm.

2.6. Protein content BCA assay

Protein concentration of wild type tPA (wt tPA) and PEGylated tPA variants were determined using Pierce™ BCA Protein Assay Kit (ThermoFisher Scientific, Karlsruhe, Germany) and measured according to manufacturer's instructions at $\lambda = 562$ nm using Tecan Reader Infinite M Plex (Tecan Group, Maennedorf, Switzerland). The measurement was performed in triplicate.

2.7. Degree of PEGylation

The degree of PEGylation was examined by determination of the mass measured by MALDI mass spectra as previously described [22]. In short, 15–40 μg of the protein variants were desalted by Sep-Pak Vac C18 cartridges (Waters GmbH, Eschborn, Germany) and lyophilized at –100 °C, 0.001 mbar. Burker Protein II standard was used as external

calibration. The protein variants were examined after double layer preparation using sinapinic acid solution.

2.8. Trypsin in-gel digest

For Trypsin in-gel digest, 0.8 μg of wt tPA, PEG-Ser1-tPA and PEG-Cys83-tPA were diluted with 4x NuPAGE Sample buffer. Samples were incubated with 50 mM dithiothreitol at 70 °C for 10 min before 120 mM iodoacetamide was added. The pH was adjusted to 7–8 and the samples were stored at room temperature for 20 min in the dark.

The samples were transferred to a gradient gel (4–20 % acrylamide) and SDS-Page was performed. Subsequently, the gel was stained with Coomassie blue G-250 and the indicated protein bands were cut out precisely (Figure S2**A**). Separate bands were destained with 400 μL of destaining buffer (70 % 100 mM ammonium bicarbonate, 30 % ACN) for 10 min. Then, the buffer was replaced with 400 μL equilibration buffer (100 mM ammonium bicarbonate, pH 8). After 10 min, gel pieces were dehydrated with 200 μL ACN for 5 min and dried by vacuum centrifugation.

Tryptic digests were performed shortly before liquid chromatography – mass spectrometry (LCMS) analysis with 0.1 μg trypsin per gel band overnight at 37 °C in equilibration buffer. After removing the supernatant, peptides were extracted from the gel slices with 5 % formic acid, and extracted peptides were pooled with the supernatant.

2.9. NanoLC-MS/MS (tandem mass spectrometry) analysis of in-gel digest samples

NanoLC-MS/MS analyses were performed on a LTQ-Orbitrap Velos Pro (Thermo Fisher, Karlsruhe, Germany) equipped with a PicoView Ion Source (New Objective, Littleton, MA) and coupled to an EASY-nLC 1000 (Thermo Fisher, Karlsruhe, Germany). Peptides were loaded on a trapping column (2 cm × 150 μm ID, PepSep) and separated on a capillary column (30 cm × 150 μm ID, PepSep) both packed with 1.9 μm C18 ReproSil and separated with a 30 min linear gradient from 3 % to 30 % ACN and 0.1 % formic acid and a flow rate of 500 nl/min.

MS scans were acquired in the Orbitrap analyzer with a resolution of 30,000 at *m/z* 400, MS/MS scans were acquired in the Orbitrap analyzer with a resolution of 7500 at *m/z* 400 using HCD (higher-energy C-trap dissociation) fragmentation with 30 % normalized collision energy. A TOP5 data-dependent MS/MS method was used; dynamic exclusion was applied with a repeat count of 1 and an exclusion duration of 15 s; singly charged precursors were excluded from selection. Minimum signal threshold for precursor selection was set to 5x104. Predictive automatic gain control (AGC) was used with AGC target a value of 106 for MS scans and 5x104 for MS/MS scans. Lock mass option was applied for internal calibration in all runs using background ions from protonated decamethylcyclopentasiloxane (*m/z* 371.10124).

2.10. MS data analysis of in-gel digest samples

Database search was performed against the protein sequence of human tPA with PEAKS Xpro software (Bioinformatics Solutions Inc., Waterloo, Canada) with the following parameters: peptide mass tolerance: 10 ppm, MS/MS mass tolerance: 0.02 Da, enzyme: Trypsin with [D \P], variable modifications: Acetylation (Protein N-term), Oxidation (M); fixed modifications: Carbamidomethylation (C), Pyro-glu from Q. Results were filtered to 1 % PSM-FDR by target-decoy approach.

2.11. Protein integrity

The structural integrity of tPA after conjugation with PEG were verified by circular dichroism (CD). CD Spectra of wt tPA (3.13 μM), PEG-Ser1-tPA (2.28 μM), PEG-Cys83-tPA (2.37 μM) and bPEG-Cys83-tPA (2.35 μM) in 25 mM acetate buffer pH 5 with 0.5 M NaCl were recorded on a Jasco J-1500CD spectrometer (Jasco Deutschland GmbH, Pfungstadt, Germany) in 0.1 cm quarz glass cuvettes.

2.12. Dynamic light scattering

The hydrodynamic size of wt tPA and PEGylated tPA variants were measured in PBS at a protein concentration of 0.2 to 0.3 mg/mL using Zetasizer Ultra Red from Malvern Panalytical (Kassel, Germany). The sample volume of 5 μL was measured using glass capillary cuvettes in four technical replicates at a scattering angle of 90°. The number-weighted size distribution was used to compare the samples.

2.13. Determination of proteolytic activity of tPA by fluorescence activity assay

The enzyme activities of wt tPA and PEGylated tPA variants were measured by mixing with 100 μM prewarmed Glutaryl-Gly-Arg-AMC substrate dissolved in 0.1 M Tris-HCl buffer pH 8.5 containing 0.02 % Tween 80 [23]. After incubation at 37 °C for 20 min, the reaction was stopped by adding 2 % SDS solution. Fluorescence intensity of proteolytically cleaved AMC was measured at emission and excitation wavelengths of 455 and 383 nm at 37 °C in Tecan Reader Infinite M Plex. Measurements were performed in triplicate.

2.14. PAI-1 resistance

The resistance of the PEGylated tPA variants against PAI-1 were determined by incubating 15 nM of PEG-Ser1-tPA, PEG-Cys83-tPA, *b*PEG-Cys83-tPA and wt tPA with various concentrations of PAI-1 for one hour at 37 °C in TBS buffer (50 mM Tris-HCl, 150 mM NaCl, pH 7.4). Then, T2943 substrate was added to a final concentration of 0.6 mM, and the residual enzyme activity was immediately determined by spectrophotometric measurement of the initial p-nitroanilide release rate at 405 nm for 45 min at 37 °C, measured in triplicate in Tecan Reader Infinite M Plex [24]. In addition, the second-order association rate constants (k_1) for the inhibition of the PEGylated tPA variants by PAI-1 were determined as previously described [25]. Therefore, 400 nM of PEG-Ser1-tPA, PEG-Cys83-tPA, *b*PEG-Cys83-tPA and wt tPA were incubated with a 1.2-fold molar excess of PAI-1 in the TBS buffer for 60 s. The reactions were stopped by dilution with TBS buffer containing 200 μM chromogenic substrate T2943 and the residual enzyme activity was determined at 405 nm for 15 min at 37 °C as described above. The second-order association rate constant (k_1) was obtained by applying a standard equation for a second-order reaction, under conditions of slight excess of inhibitor over enzyme (see Eq. (1)).

$$k_1 \times t = \frac{1}{(I_0 - E_0)} \times \left[\ln\left(1 + \frac{(I_0 - E_0)}{E_t}\right) - \ln\left(\frac{I_0}{E_0}\right) \right] \quad (1)$$

with E_0 and I_0 as the initial concentrations of enzyme and inhibitor, respectively and E_t as the enzyme concentration at time t in seconds.

2.15. Cytotoxicity

The cytotoxicity of the PEGylated tPA variants were examined using human embryonic kidney HEK293 cells (ATCC; CRL-1573) seeded in a 96-well plate format (5000 cells/well; 100 μL per well) in Dulbecco's modified Eagle's medium supplemented with 10 % (v/v) BCS, 100 U/mL penicillin G, and 100 μg/mL streptomycin. The HEK293 cells were treated with dilution series of wt tPA as control and the tPA-variants, PEG-Ser1-tPA and PEG-Cys83-tPA, ranging from 30 nM to 1.9 pM. Appropriate concentrations of storage buffer (25 mM acetate buffer pH 5 with 0.5 M NaCl) were used as negative control. After 24 h of treatment, cells were incubated with WST-1 for 4 h at 37 °C according to manufacturer's instructions. The mitochondrial activity after incubation with the tPA variants was determined by measuring the absorbance of the soluble formazan product at 450 nm as well as background noise at 630

nm using Tecan Reader Infinite M Plex.

2.16. Statistical analysis

Statistical analysis was performed with OriginPro 2020 (OriginLab Corporation, Northampton, USA). Comparison between enzyme activities was performed using two sample *t*-test. Comparison of PAI-1 resistance and increase of hydrodynamic size was performed with analysis of variance (ANOVA). Samples with p-value < 0.05 were considered as statistically significant and are marked with an asterisk (*).

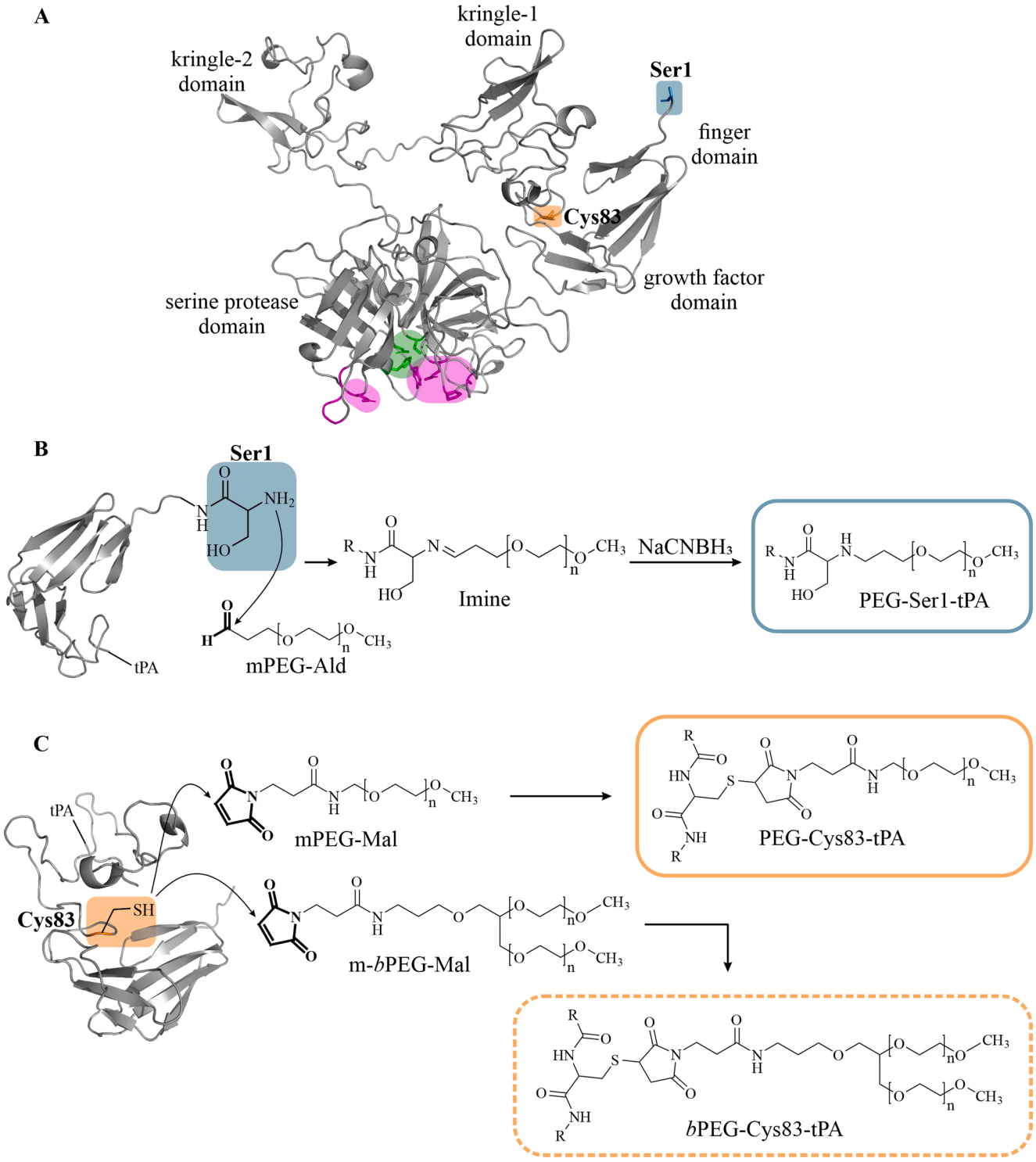

Scheme 1. (A) tPA modelled by alpha-fold (UniProt: P00750) with the five domains including Ser1 (blue) at the N-terminus, Cys83 (orange), the proteolytic site with the catalytical triad (His322, Asp371, Ser478; green) and the inhibitor binding sites (purple) [37,38]. (B) Site-specific PEGylation at the N-terminus (Ser1, blue) of tPA with mPEG-Ald by reductive amination. First step shows formation of imine intermediate at pH 5, second step the reduction with $NaCNBH_3$ to the secondary amine. (C) Site-specific PEGylation at the single-free cysteine (Cys83, orange) of tPA with mPEG-Mal or m-bPEG-Mal by maleimide reaction at pH 7.2.

3. Results and discussion

3.1. Selection of PEGylation sites

PEGylation sites of tPA were selected considering the selectivity for a single conjugation approach and its possible influence on bioactivity (Scheme 1**A**).

The first approach selectively targets the primary amine (Ser1) at the N-terminus of tPA by reductive amination at pH 5 as previously described (Scheme 1**B**) [17]. As a second approach, the surface exposed free cysteine residue Cys83 was used for thiol-maleimide reaction (Scheme 1**C**). All other cysteines in tPA are bound in disulfide bonds. Both PEGylation sites are spatially distant from the low-lying catalytic triad of tPA which consists of His322, Asp371 and Ser478 (Scheme 1**A**) to enable bioactivity of the PEGylated product [26]. In addition to conjugating linear PEG at both PEGylation sites, the thiol-maleimide reaction was also performed with 2-arm branched PEG to investigate the effect of PEG's architecture on the steric hindrance of the PAI-binding sites.

3.2. Site-specific PEGylation and purification

The primary amine (Ser1) at the N-terminus of tPA was selectively PEGylated by reductive amination with linear mPEG-Ald. Mono-PEGylated tPA (PEG-Ser1-tPA) was separated from unreacted tPA by cation exchange chromatography, yielding in an overall purity exceeding 99 % of the PEGylated product (Fig. 1**A, B**). Reductive SDS-Page showed the increase in molar mass of PEG-Ser1-tPA compared to wt tPA (Figure S1**A**). Since precise determination of molar mass by SDS-Page is interfered by the interaction of PEG with negatively charged SDS micelles, MALDI was used to determine the degree of PEGylation and the molar mass [27]. The results showed mass increase of about 20,000 g/mol compared to wt tPA, corresponding to the mono-conjugated PEG-tPA (Fig. 1**C, D**).

The second PEGylation approach of tPA targeted the single-free cysteine (Cys83) by deploying maleimide chemistry with linear mPEG-Mal and branched m-*b*PEG-Mal. Both mono-PEGylated products (PEG-Cys83-tPA and *b*PEG-Cys83-tPA, respectively) were purified by cation-exchange chromatography. PEG-Cys83-tPA was obtained with a purity exceeding 95 % (Fig. 2**A, B**) and *b*PEG-Cys83-tPA with a purity exceeding 96 % (Fig. 3**A, B**). Similar to PEG-Ser1-tPA, the band shift of the maleimide mediated tPA conjugates occurred on the SDS-Page compared to wt tPA (**Fig. S1B, S1C**). The mass of PEG-Cys83-tPA and *b*PEG-Cys83-tPA were increased by one PEG molecule to approximately 85,000 g/mol compared to wt tPA (Fig. 2**C, D,** 3**C, D**).

The selectivity of the PEGylation site was verified by in-gel trypsin digestion of PEG-Ser1-tPA and PEG-Cys83-tPA followed by liquid chromatography – mass spectrometry of obtained peptides. PEGylated peptides cannot be measured due to their size and therefore disappear from the chromatograms compared to wt tPA. Examination of the peptides showed the underrepresentation of the N-terminal peptides (SYQVIcRDEK, SYQVIcR) for PEG-Ser1-tPA and the Cys83-containing peptide (ccEIDTR) for PEG-Cys83-tPA (**Figure S2**). This finding and the degree of PEGylation from the MALDI results suggest site-specific modification of tPA for both types of conjugation chemistries used.

3.3. Structural integrity and hydrodynamic size of PEGylated tPA variants

The structural integrity of the PEGylated tPA variants was investigated by circular dichroism (CD). The CD spectra of the PEGylated tPA variants showed similar characteristics to those of wt tPA (**Figure S4**). In particular, the curve of the far UV CD spectra (240 nm and below) showed the random coil of the secondary structure from the peptide bond region and suggests structure maintenance after PEGylation [28] (Fig. 4**A**).

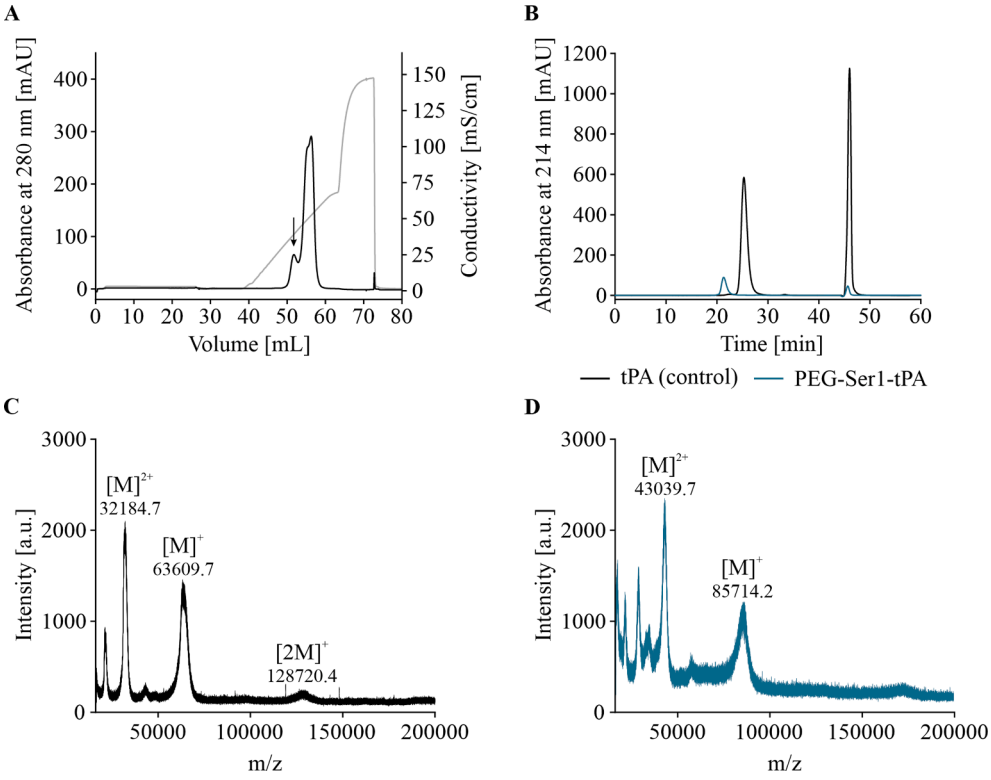

Fig. 1. Purification of PEG-Ser1-tPA. (A) Chromatogram of CEX purification step showing absorbance at 280 nm (black) and conductivity (gray). Arrow marks conjugated tPA. (B) SEC-HPLC chromatogram of tPA as control (black) and PEG-Ser1-tPA (blue). (C) MALDI-mass spectrum of tPA as control. (D) MALDI-mass spectrum of PEG-Ser1-tPA.

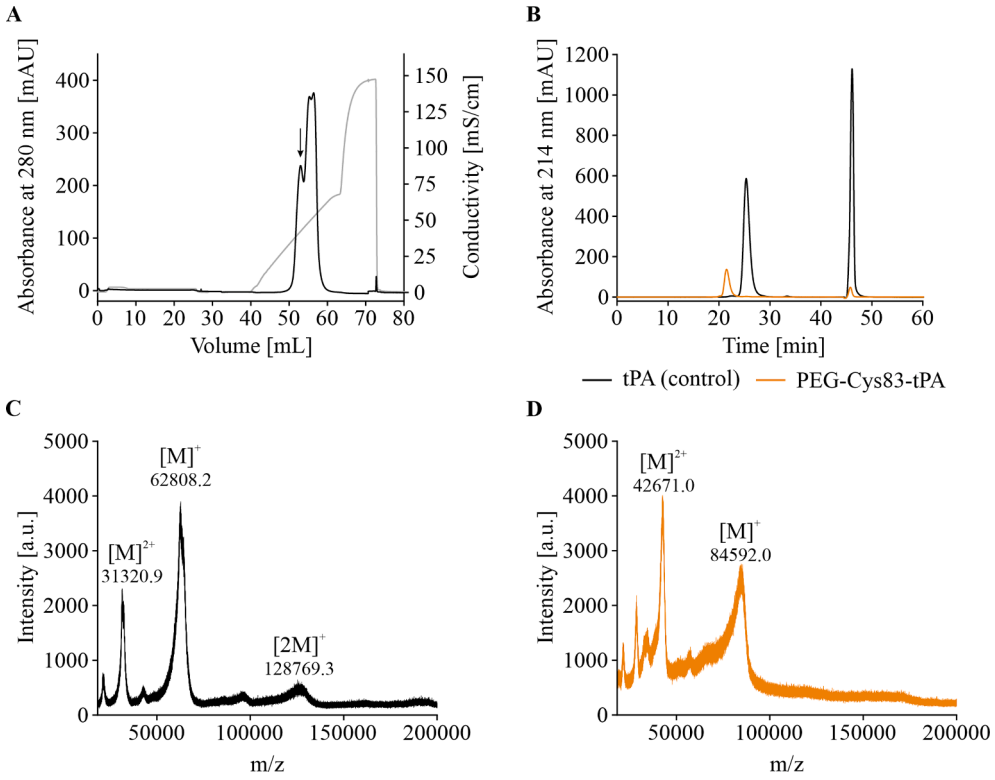

Fig. 2. Purification of PEG-Cys83-tPA. (A) Chromatogram of CEX purification step showing absorbance at 280 nm (black) and conductivity (gray). Arrow marks conjugated tPA. (B) SEC-HPLC chromatogram of tPA as control (black) and PEG-Cys83-tPA (orange). (C) MALDI-mass spectrum of tPA as control. (D) MALDI-mass spectrum of PEG-Cys83-tPA.

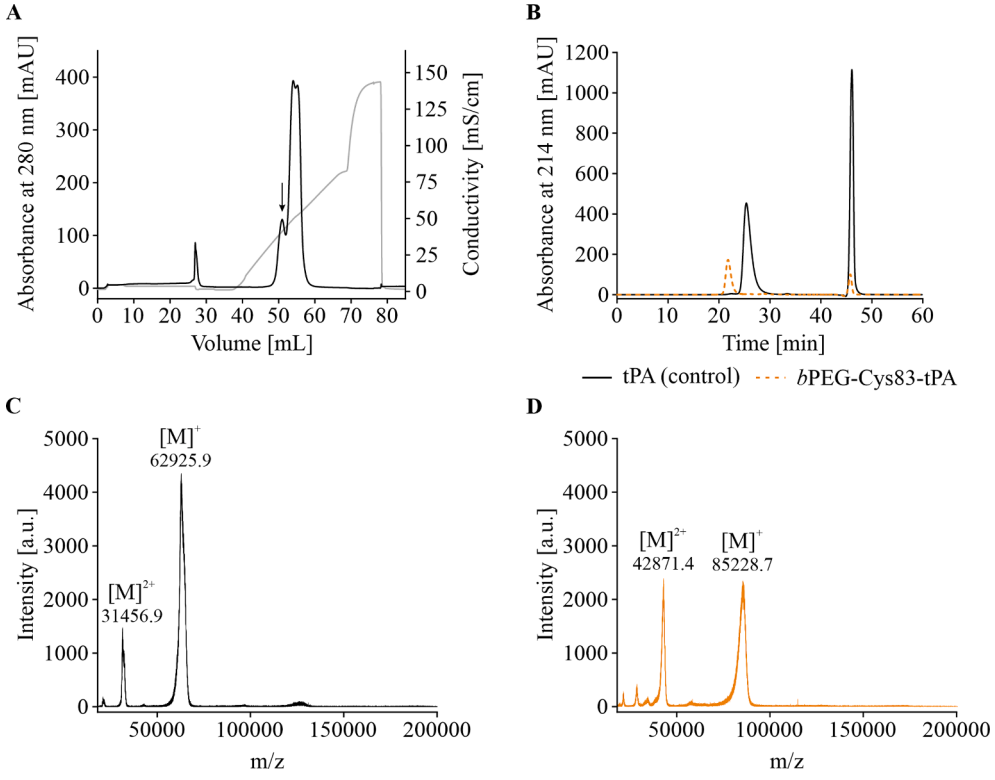

Fig. 3. Purification of *b*PEG-Cys83-tPA. (A) Chromatogram of CEX purification step showing absorbance at 280 nm (black) and conductivity (gray). Arrow marks conjugated tPA. (B) SEC-HPLC chromatogram of tPA as control (black) and *b*PEG-Cys83-tPA (orange dashed). (C) MALDI-mass spectrum of tPA as control. (D) MALDI-mass spectrum of *b*PEG-Cys83-tPA.

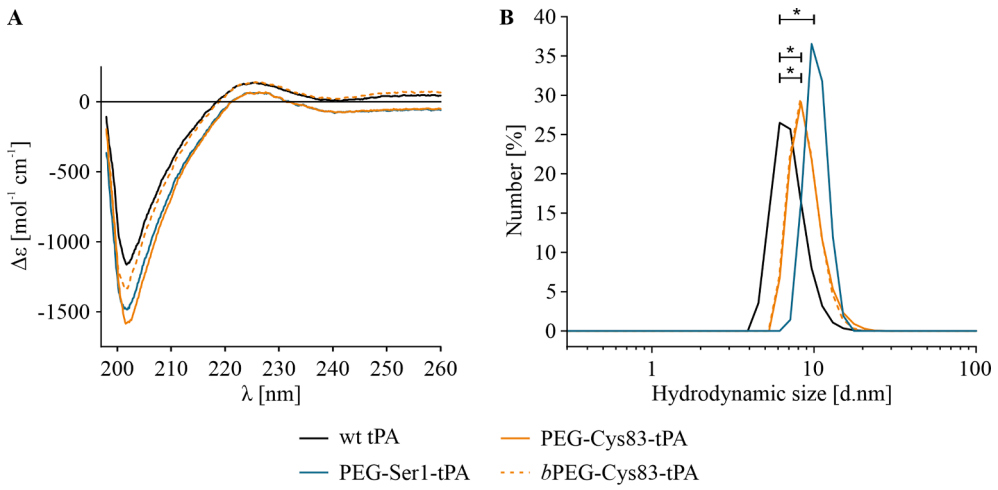

Fig. 4. (A) Circular dichroism spectra (195 nm–260 nm) of wt tPA (black), PEG-Ser1-tPA (blue), PEG-Cys83-tPA (orange) and *b*PEG-Cys83-tPA (orange dashed). (B) The number weighted size distribution of PEG-Ser1-tPA (blue), PEG-Cys83-tPA (orange) and *b*PEG-Cys83-tPA (orange dashed) compared to wt tPA (black) measured by dynamic light scattering (DLS) shows the increase in hydrodynamic size after conjugation with PEG (20 kDa). Measurements were performed at a scattering angle of 90° and were performed in quadruplicate.

The hydrodynamic size of PEGylated tPA was determined by dynamic light scattering (Fig. 4**B**, **Figure S3**). The hydrodynamic size of unconjugated tPA was 7.16 ± 0.82 nm (**Table S1**). After PEGylation, the hydrodynamic size increased statistically significant to 10.51 ± 1.05 nm (PEG-Ser1-tPA), 9.76 ± 1.41 nm (PEG-Cys83-tPA) and 9.50 ± 0.37 nm (*b*PEG-Cys83-tPA), respectively.

3.4. Determination of remaining proteolytic activity of PEGylated tPA variants

The remaining bioactivity of the PEGylated tPA variants was assessed by proteolytic activity per milligram protein and compared to wild type tPA. For this purpose, protein quantification was first performed with bicinchoninic acid (BCA), and proteolytic activity was subsequently determined using a commercial fluorescence substrate assay. Thereby, proteolytic activity is expressed in international units [IU], referenced to the WHO Reference Material II for rt-PA as described in the European Pharmacopoeia monograph for Alteplase for injection (Ph.Eur. 11.2, 1170 (07/2013)).

Compared to wild type tPA, the activity of PEG-Ser1-tPA was reduced to 68 %. In contrast, the maleimide conjugated tPA variants showed higher activities with 96 % for *b*PEG-Cys83-tPA and, in the case of PEG-Cys83-tPA, no statistically significant decrease in activity (Fig. 5**A**).

Since the integrity of the proteins is maintained, as demonstrated above, the difference in the remaining activity could be attributed to the shielding of the catalytic triad from the substrate, depending on the PEGylation site (Scheme 1).

3.5. PAI-1 resistance of PEGylated tPA variants

PAI-1 binds to the catalytic triad of tPA in a two-step mechanism. In the first step, tPA and PAI-1 associate reversibly, followed by slow irreversible complex formation, leading to rapid metabolization in the

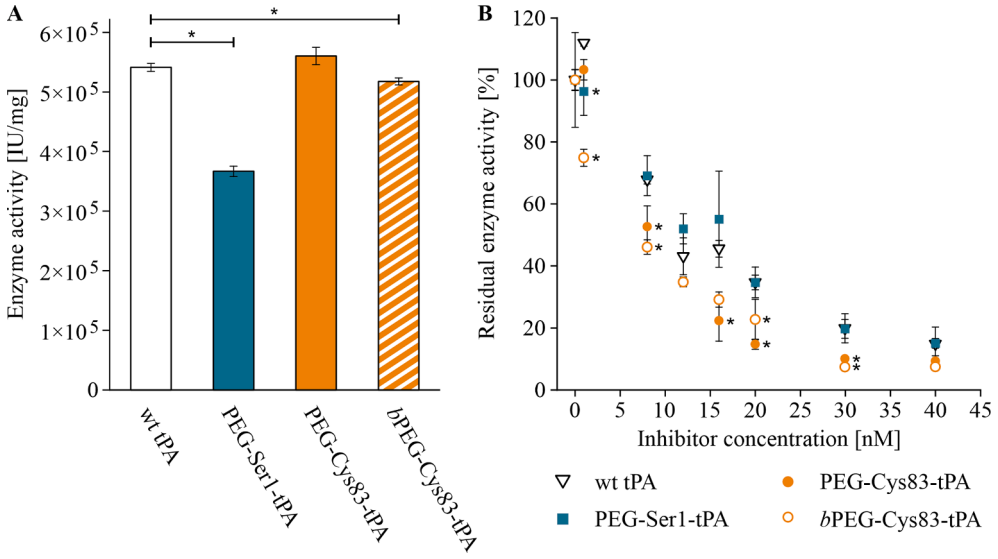

Fig. 5. Proteolytic enzyme activity of PEG-Ser1-tPA (blue), PEG-Cys83-tPA (orange solid) and *b*PEG-Cys83-tPA (orange striped; orange open) compared to wild type tPA (open, black). (A) Enzyme activity in international units per milligram of protein. Protein amounts were measured by BCA assay, enzyme activities were determined by fluorescence substrate activity assay. (B) PAI-1 resistance assessed by residual enzyme activity depending on inhibitor concentrations. Determination of enzymatic activity using chromogenic substrate T2943. All measurements were performed in triplicate, asterisks mark statistically significant differences to wt tPA.

liver [29,30]. tPA has multiple binding sites on the surface interacting with the reactive center loop (RCL) of PAI-1 [26,31]. Therefore, the effect of PEGylations on shielding tPA from PAI-1 and disrupting interactions with these binding sites was investigated considering both the PEGylation site and PEG architecture. The residual activity of the PEGylated tPA variants after one hour incubation with PAI-1 showed a similar correlation with the concentration of the inhibitor as wt tPA (Fig. 5**B**). In contrast, the second order associated rate constants behaved differently. PEG-Ser-1 tPA showed slightly faster inhibition by PAI-1 than wt tPA, whereas PEG-Cys83-tPA and *b*PEG-Cys83-tPA exhibited 2-fold slower inhibition (Table 1). This suggests that PEGylation at the single-free cysteine of tPA masks PAI-1 binding sites with some molecular reduction of interaction.

3.6. Cytotoxicity of PEGylated tPA variants

The cytotoxicity of the PEGylated tPA variants, PEG-Ser1-tPA and PEG-Cys83-tPA, were assessed by mitochondrial activity of human embryonic cells after incubation with the tPA conjugates. The PEGylated tPA variants showed no difference to wt tPA at all concentrations (**Figure S5**).

In this study, we compared two strategies of site-specific PEGylation for tPA. PEGylation was successfully performed by both chemistries, reductive amination at the N-terminus and by thiol-maleimide reaction, resulting in mono-PEGylated products. Thiol-maleimide mediated conjugation with linear PEG resulted in PEGylated tPA without loss of bioactivity and a 2-fold decreased binding kinetics to the inhibitor PAI-1. Although bioactivity of the PEGylated product with cysteine modification was unaltered as prerequisite for therapeutic use, shielding of tPA to the inhibitor PAI-1 should be further improved. Conceptionally, the ideal tPA therapeutic would benefit from long circulation, unaltered enzymatic activity, and low binding to its blood derived inhibitor PAI-1. To optimize the steric hindrance of PAI-1 to tPA, initial attempts were made to investigate bulkier 2-armed PEG. The resulting conjugate showed similar bioactivity but no improvement in inhibition by PAI-1 compared to the use of linear PEG. Thus, future studies are needed to extend our conjugation strategy of wild type tPA using even larger or bulkier PEG material, e.g. 40 kDa or multi-branched PEG polymers for conjugation of tPA at Cys83, to potentially yield in an improved coverage of the PAI–1 – tPA binding interphase. Another approach may include protein engineering strategies. One option is the decoration of PEG in the proximity to the PAI-1 binding site (Glu326, Tyr368, Ala419, Pro422, Gln475) with genetic code expansion for site-specific incorporation of an unnatural amino acid in tPA for polymer attachment as previously demonstrated [31,32]. However, this approach demands recombinant manufacturing of a tPA mutant with potential safety risks as demonstrated for Tenecteplase [10].

Regarding the *in vivo* stability of tPA-maleimide conjugates with free thiols in blood, the bioconjugates should withstand at least the time of repetitive hepatic exposure. Other studies show half-lives of 20 to 80 h for retro reactions of maleimide thiol adducts [33,34]. For instance, Shen et al. confirmed the partial transfer of their conjugate to albumin in plasma after 96 h [35]. Since free tPA is hepatically cleared within a few minutes, the stability of the conjugates during this time window can be assumed, but should further be verified in a future pharmacokinetic (PK) study.

From a PK perspective, fully bioactive PEG-Cys83-tPA or *b*PEG-Cys83-tPA with a hydrodynamic size of 10 nm should be tested in future *in vivo* studies to assess if PEG attachment reduces interactions with mannose and low density lipoprotein (LDP) receptors, responsible for the fast hepatic clearance of free tPA [36].

4. Conclusion

This work presents two different bioconjugation chemistries and purification strategies for site directed PEGylation of human recombinant tPA to address its rapid clearance from blood. PEGylation by maleimide chemistry with linear or branched PEG and reductive amination at the N-terminus with linear PEG was effective, yielding mono-PEGylated tPA products. Bioactivities of the maleimide based PEGylated tPAs (PEG-Cys83-tPA, *b*PEG-Cys83-tPA) were on par to the wild-type with 2-fold reduced binding kinetics to the inhibitor PAI-1. Demonstrating hydrodynamic diameters of 10 nm, PEG-Cys83-tPA and *b*PEG-Cys83-tPA are suitable candidates for future pharmacokinetic and pharmacodynamic studies.

Table 1
Second-order association rate constants (k_1) for the interaction of tPA variants with PAI-1.

tPA variants	k_1 (L/mol·s)	Resistance ability (fold)
tPA (control)	$4.09 \pm 0.17 \times 10^5$	1.00
PEG-Ser1-tPA	$4.52 \pm 0.05 \times 10^5$	0.90
PEG-Cys83-tPA	$2.04 \pm 0.20 \times 10^5$	2.01
*b*PEG-Cys83-tPA	$2.09 \pm 0.63 \times 10^5$	1.95

Declaration of Competing Interest

The authors declare that they have no known competing financial interests or personal relationships that could have appeared to influence the work reported in this paper.

Data availability

Data will be made available on request.

Acknowledgements

We sincerely thank Dr. Andreas Schlosser and Stephanie Lamer (Rudolf Virchow Zentrum, University of Würzburg, Germany) for the nanoLC-MS/MS measurements. We sincerely thank Dr. Juliane Adelmann (Institute of Organic Chemistry, University of Würzburg, Germany) for the MALDI measurements. We thank the European Union's Horizon 2020 research and innovation programme under grant agreement No 952152, project ANGIE (Magnetically steerable wireless Nanodevices for the targeted delivery of therapeutic agents in any vascular region of the body) for kindly supporting out research. A.N.-K. thanks the German Research Foundation (DFG) for an Emmy-Noether Fellowship (NO1459/1-1) and the Hector Fellow Academy (HFA) for financial support. J.N. thanks the HFA for a Ph.D. scholarship.

Appendix A. Supplementary material

The following files are available free of charge: protein sequence of recombinant tissue-type-plasminogen activator, SDS-Page after CEX purification, trypsin in-gel digestion with sequence coverage and LC/MS analysis, single measurements of number weighted size distribution and hydrodynamic size, circular dichroism spectra (195 nm to 400 nm), cytotoxicity and serum stability of PEGylated tPA variants. Supplementary data to this article can be found online at https://doi.org/10.1016/j.ejpb.2023.09.017.

References

[1] X. Wang, et al., Human plasminogen catalytic domain undergoes an unusual conformational change upon activation, J. Mol. Biol. 295 (2000) 903–914, https://doi.org/10.1006/jmbi.1999.3397.
[2] D. Pennica, et al., Cloning and expression of human tissue-type plasminogen activator cDNA in E. coli, Nature 301 (1983) 214–221, https://doi.org/10.1038/301214a0.
[3] B. Wiman, D. Collen, Molecular mechanism of physiological fibrinolysis, Nature 272 (1978) 549–550, https://doi.org/10.1038/272549a0.
[4] H.P. Adams Jr., et al., Guidelines for the early management of adults with ischemic stroke: a guideline from the American Heart Association/American Stroke Association Stroke Council, Clinical Cardiology Council, Cardiovascular Radiology

and Intervention Council, and the Atherosclerotic Peripheral Vascular Disease and Quality of Care Outcomes in Research Interdisciplinary Working Groups: the American Academy of Neurology affirms the value of this guideline as an educational tool for neurologists, Stroke 38 (2007) 1655–1711, https://doi.org/10.1161/STROKEAHA.107.181486.

[5] E.K. Kruithof, C. Tran-Thang, A. Ransijn, F. Bachmann, Demonstration of a fast-acting inhibitor of plasminogen activators in human plasma, Blood 64 (1984) 907–913, https://doi.org/10.1182/blood.V64.4.907.907.

[6] M. Verstraete, H. Bounameaux, F. De Cock, F. Van de Werf, D. Collen, Pharmacokinetics and systemic fibrinogenolytic effects of recombinant human tissue-type plasminogen activator (rt-PA) in humans, J. Pharmacol. Exp. Ther. 235 (1985) 506–512.

[7] E.J.P. Brommer, F.H.M. Derkx, M.A.D.H. Schalekamp, G. Dooijewaard, M.M.v. d. Klaauw, Renal and hepatic handling of endogenous tissue-type plasminogen activator (t-PA) and its inhibitor in man, Thromb. Haemost. 59 (1988) 404–411, https://doi.org/10.1055/s-0038-1647505.

[8] W.M. Clark, et al., Recombinant tissue-type plasminogen activator (Alteplase) for ischemic stroke 3 to 5 hours after symptom onset. The ATLANTIS Study: a randomized controlled trial. Alteplase thrombolysis for acute noninterventional therapy in ischemic stroke, J. Am. Med. Assoc. 282 (1999) 2019–2026, https://doi.org/10.1001/jama.282.21.2019.

[9] D. Collen, H.R. Lijnen, P.A. Todd, K.L. Goa, Tissue-type plasminogen activator. A review of its pharmacology and therapeutic use as a thrombolytic agent, Drugs 38 (1989) 346–388, https://doi.org/10.2165/00003495-198938030-00003.

[10] C. Marti, et al., Systemic thrombolytic therapy for acute pulmonary embolism: a systematic review and meta-analysis, Eur. Heart J. 36 (2015) 605–614, https://doi.org/10.1093/eurheartj/ehu218.

[11] S. Jevsevar, M. Kunstelj, V.G. Porekar, PEGylation of therapeutic proteins, Biotechnol. J. 5 (2010) 113–128, https://doi.org/10.1002/biot.200900218.

[12] Q. Mu, T. Hu, J. Yu, Molecular insight into the steric shielding effect of PEG on the conjugated staphylokinase: biochemical characterization and molecular dynamics simulation, PLoS One 8 (2013) e68559.

[13] A.C. Braun, M. Gutmann, T. Luhmann, L. Meinel, Bioorthogonal strategies for site-directed decoration of biomaterials with therapeutic proteins, J. Control. Release 273 (2018) 68–85, https://doi.org/10.1016/j.jconrel.2018.01.018.

[14] J.K. Dozier, M.D. Distefano, Site-specific PEGylation of therapeutic proteins, Int. J. Mol. Sci. 16 (2015) 25831–25864.

[15] O. Kinstler, G. Molineux, M. Treuheit, D. Ladd, C. Gegg, Mono-N-terminal poly (ethylene glycol)–protein conjugates, Adv. Drug Deliv. Rev. 54 (2002) 477–485, https://doi.org/10.1016/S0169-409X(02)00023-6.

[16] M.J. Roberts, M.D. Bentley, J.M. Harris, Chemistry for peptide and protein PEGylation, Adv. Drug Deliv. Rev. 54 (2002) 459–476, https://doi.org/10.1016/s0169-409x(02)00022-4.

[17] M. Tully, et al., Linear Polyglycerol for N-terminal-selective Modification of Interleukin-4, J. Pharm. Sci. 111 (2022) 1642–1651, https://doi.org/10.1016/j.xphs.2021.10.032.

[18] A.M. Wolkersdorfer, et al., PEGylation of human vascular endothelial growth factor, ACS Biomater Sci. Eng. (2023), https://doi.org/10.1021/acsbiomaterials.3c00253.

[19] H.J. Berger, S. Pizzo, Preparation of polyethylene glycol-tissue plasminogen activator adducts that retain functional activity: characteristics and behavior in three animal species, Blood 71 (1988) 1641–1647, https://doi.org/10.1182/blood.V71.6.1641.1641.

[20] R. Liebner, M. Meyer, T. Hey, G. Winter, A. Besheer, Head to head comparison of the formulation and stability of concentrated solutions of HESylated versus PEGylated anakinra, J. Pharm. Sci. 104 (2015) 515–526, https://doi.org/10.1002/jps.24253.

[21] H.-A. Chen, Y.-H. Ma, T.-Y. Hsu, J.-P. Chen, Preparation of peptide and recombinant tissue plasminogen activator conjugated poly(lactic-co-glycolic acid) (PLGA) magnetic nanoparticles for dual targeted thrombolytic therapy, Int. J. Mol. Sci. 21 (2020) 2690.

[22] A.M. Wolkersdorfer, *et al.* Deprivation of arginine and lysine interferes with growth of patient-derived tumor xenografts. *bioRxiv*, 2023.2001.2017.524398, 2023, doi: 10.1101/2023.01.17.524398.

[23] G.D.J. Green, Poly-lysines as modifiers of one- and two-chain tissue-type plasminogen activator activity, Thromb. Res. 44 (1986) 849–857, https://doi.org/10.1016/0049-3848(86)90030-7.

[24] F. Bachmann, I.E.K. Kruithof, in: *Seminars in thrombosis and hemostasis.* 6-17 (Copyright© 1984 by Thieme Medical Publishers, Inc.).

[25] J. Keijer, et al., On the target specificity of plasminogen activator inhibitor 1: the role of heparin, vitronectin, and the reactive site, Blood 78 (1991) 1254–1261, https://doi.org/10.1182/blood.V78.5.1254.1254.

[26] W.F. Bennett, et al., High resolution analysis of functional determinants on human tissue-type plasminogen activator, J. Biol. Chem. 266 (1991) 5191–5201, https://doi.org/10.1016/S0021-9258(19)67773-2.

[27] C.Y. Zheng, G. Ma, Z. Su, Native PAGE eliminates the problem of PEG–SDS interaction in SDS-PAGE and provides an alternative to HPLC in characterization of protein PEGylation, Electrophoresis 28 (2007) 2801–2807, https://doi.org/10.1002/elps.200600807.

[28] M. Bayat, et al., Stabilizing osmolytes' effects on the structure, stability and function of tc-tenecteplase: A one peptide bond digested form of tenecteplase, Int. J. Biol. Macromol. 130 (2019) 863–877, https://doi.org/10.1016/j.ijbiomac.2019.03.035.

[29] H.L. Dauerman, P.B. Gogo, B.E. Sobel, in: David L. Brown, (ed.) *Cardiac Intensive Care,* Elsevier, 2019, pp. 103–116.e105.

[30] C.M. Hekman, D.J. Loskutoff, Kinetic analysis of the interactions between plasminogen activator inhibitor 1 and both urokinase and tissue plasminogen activator, Arch. Biochem. Biophys. 262 (1988) 199–210, https://doi.org/10.1016/0003-9861(88)90182-8.

[31] S. Peng, et al., tPA Point Mutation at Autolysis Loop Enhances resistance to PAI-1 inhibition and catalytic activity, Thromb. Haemost. 119 (2019) 77–86, https://doi.org/10.1055/s-0038-1676518.

[32] T. Lühmann, et al., Interleukin-4-clicked surfaces drive M2 macrophage polarization, Chembiochem 17 (2016) 2123–2128, https://doi.org/10.1002/cbic.201600480.

[33] A.D. Baldwin, K.L. Kiick, Tunable degradation of maleimide-thiol adducts in reducing environments, Bioconjug. Chem. 22 (2011) 1946–1953, https://doi.org/10.1021/bc200148v.

[34] S.C. Alley, et al., Contribution of linker stability to the activities of anticancer immunoconjugates, Bioconjug. Chem. 19 (2008) 759–765, https://doi.org/10.1021/bc7004329.

[35] B.-Q. Shen, et al., Conjugation site modulates the in vivo stability and therapeutic activity of antibody-drug conjugates, Nat. Biotechnol. 30 (2012) 184–189, https://doi.org/10.1038/nbt.2108.

[36] W.L. Chandler, et al., Clearance of tissue plasminogen activator (TPA) and TPA/plasminogen activator inhibitor type 1 (PAI-1) complex, Circulation 96 (1997) 761–768, https://doi.org/10.1161/01.CIR.96.3.761.

[37] J. Jumper, et al., Highly accurate protein structure prediction with AlphaFold, Nature 596 (2021) 583–589, https://doi.org/10.1038/s41586-021-03819-2.

[38] M. Varadi, et al., AlphaFold protein structure database: massively expanding the structural coverage of protein-sequence space with high-accuracy models, Nucleic Acids Res. 50 (2022) D439–D444, https://doi.org/10.1093/nar/gkab1061.